

# Multispectral image compression with band ordering and wavelet transforms

Ahmed Hagag · Mohamed Amin ·  
Fathi E. Abd El-Samie

Received: 23 January 2013 / Revised: 14 May 2013 / Accepted: 31 May 2013 / Published online: 28 June 2013  
© Springer-Verlag London 2013

**Abstract** In this paper, a new compression technique aiming at reducing the size of storage of multispectral images and maintaining at the same time the high-quality reconstruction is presented. An optimal multispectral band ordering process is applied before compression, and then, the dual-tree discrete wavelet transform is used in the spectral dimension, and the 2D discrete wavelet transform is used in the spatial dimensions. Finally, a simple Huffman coder is used for compression. Landsat ETM+ images are used for experiments. Experimental results demonstrate that the proposed technique has better performance than JPEG, JPEG2000, SPIHT, and JPEG2000 with a 3D dual-tree transformation.

**Keywords** Multispectral compression · Landsat · DDWT · DWT · Multispectral band ordering

## 1 Introduction

Satellite images are of interest for a large number of applications, such as geology, earth-resource management, pollution monitoring, meteorology, and military surveillance.

---

A. Hagag (✉)  
Department of Information Technology, Faculty of Information  
Technology, Egyptian E-Learning University, Dokki,  
Giza 12611, Egypt  
e-mail: ahagag88@gmail.com

M. Amin  
Department of Mathematics, Faculty of Science,  
Menoufia University, Shebin El-Koom 32511, Egypt  
e-mail: mohamed\_amin110@yahoo.com

F. E. Abd El-Samie  
Department of Electronics and Electrical Communications, Faculty  
of Electronic Engineering, Menoufia University, Menouf 32952, Egypt  
e-mail: fathi\_sayed@yahoo.com

As a consequence, there is a constant growth both in the number and in the performance of satellite image facilities, which produce larger and larger amounts of data that have to be transmitted, processed, and stored efficiently. Thus, it is common to include data compression as a part of the distribution system for satellite imagery. The problem stems from the size of the raw images considered, where the amount of data to be managed further increases with the number of bands. The result is a large amount of data organized in three dimensions. Two dimensions are the spatial dimensions, and the third is the spectral dimension indexed by  $\lambda$ .

A satellite image has both spatial and spectral resolutions. Data with two spectral bands (or channels) per pixel are called dual-band data. Data with three to several (perhaps 6–10) bands are termed multispectral data, and data with more bands are termed hyper-spectral data [1–6].

Multispectral data are typically arranged as a 3D structure as shown in Fig. 1. Each plane is a band, and it consists of rows and columns of pixels. We can interpret each plane of Fig. 1 as an image (pixels displayed in a spatial relationship to one another) and each column as a spectrum (variations within pixels as functions of wavelength).

Multispectral image compression is one of the important fields that have useful applications in data storage and transmission. It is necessary in any instance where images need to be stored, transmitted, or viewed quickly and efficiently. In this paper, an efficient multispectral image compression technique is presented and compared with traditional compression techniques. Landsat ETM+ multispectral images are used for the validation of the proposed technique. The rest of the paper is organized as follows. Traditional multispectral compression techniques are discussed in Sect. 2. The proposed technique is presented in Sect. 3. Experimental results are presented in Sect. 4. Finally, conclusions are drawn in the last section.

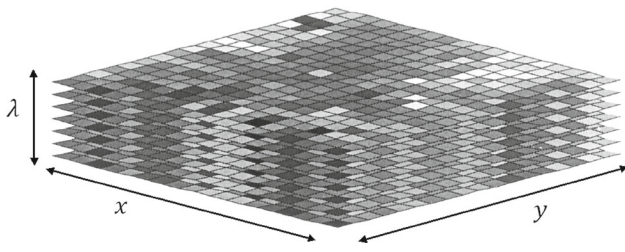


Fig. 1 The 3D structure of multispectral data

### 2 Traditional multispectral compression techniques

Multispectral image compression needs the use of 3D transformations to benefit from the relationship between bands. The 3D compression techniques are generally extended from their 2D counterparts. The techniques of particular interest that will be used in our investigation are the Joint Photographic Experts Group 2000 (JPEG2000) which is an extended version of the Joint Photographic Experts Group (JPEG), the 3D Set Partitioning In Hierarchical Trees (SPIHT) which is extended from the 2-D SPIHT, and the dual-tree discrete wavelet transform (DDWT) [7–12].

#### 2.1 JPEG compression

JPEG compression uses the 3D discrete cosine transform (DCT). There are two classes of encoding and decoding processes: lossy and lossless. Those based on the DCT [13] are lossy, thereby allowing substantial compression to be achieved, while producing a reconstructed image with high visual fidelity to the encoder source image.

It was suggested in [1] that there is a possibility of extending the DCT to three dimensions as in Eqs. (1) and (2) [1] and applying it to the compression of multispectral data. The extension is straightforward. Simply partition a large set of multispectral data into cubes of  $8 \times 8 \times 8$  pixels, apply the 3D DCT to each cube, collect the resulting transform coefficients in a zigzag sequence, quantize them, and encode the results with an entropy coder such as the Huffman coder [14].

$$G_{ijk} = \sqrt{\frac{2^3}{n^3}} C_i C_j C_k \sum_{x=0}^{n-1} \sum_{y=0}^{n-1} \sum_{z=0}^{n-1} p_{xyz} \cos \left[ \frac{(2x+1)i\pi}{2n} \right] \cos \left[ \frac{(2y+1)j\pi}{2n} \right] \cos \left[ \frac{(2z+1)k\pi}{2n} \right], \tag{1}$$

for  $0 \leq i, j, k \leq n - 1$  and

$$C_f = \begin{cases} 1/\sqrt{2} & \text{for } f = 0 \\ 1 & \text{for } f > 0 \end{cases}$$

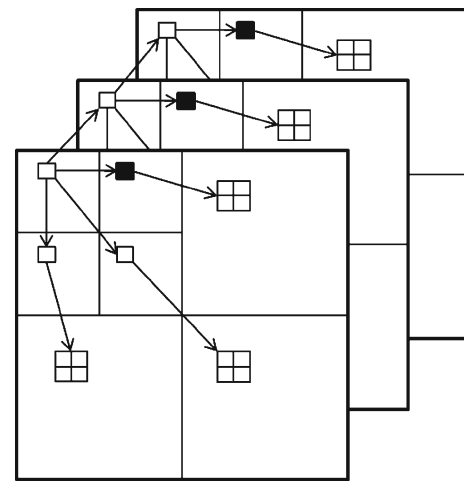


Fig. 2 Tree structure used in the 3D SPIHT algorithm

and the inverse 3D DCT is

$$p_{xyz} = \sqrt{\frac{2^3}{n^3}} \sum_{i=0}^{n-1} \sum_{j=0}^{n-1} \sum_{k=0}^{n-1} C_i C_j C_k G_{ijk} \cos \left[ \frac{(2x+1)i\pi}{2n} \right] \cos \left[ \frac{(2y+1)j\pi}{2n} \right] \cos \left[ \frac{(2z+1)k\pi}{2n} \right], \tag{2}$$

for  $0 \leq x, y, z \leq n - 1$ .

#### 2.2 SPIHT compression

SPIHT is an embedded coding algorithm that performs bit-plane coding of the wavelet coefficients [15]. In [9], two implementations of SPIHT compression are proposed. In the first, a 3D transform is taken and a simple 3D SPIHT is used. In the second, after taking a spatial wavelet transform, spectral vectors of pixels are vector quantized and a gain-driven SPIHT is used.

In [16], the Karhunen–Loève transform (KLT) is used to decorrelate the data in the spectral domain, followed by a 2D DCT in the spatial domain. After the transform, a 3D hierarchical structure is defined to run the SPIHT algorithm. Based on some preliminary experiments, the structure shown schematically in Fig. 2 was selected.

#### 2.3 JPEG2000 compression

JPEG2000 is the new ISO/IEC still-image compression standard [7,8]. It not only provides better compression performance over DCT-based JPEG, it also has other good features such as progressive transmission, region of interest (ROI) encoding, and error resilience.

The JPEG2000 encoder consists of four main stages: DWT, scalar quantization, and two tiers of block coding [17].

**Fig. 3** **a** Original bands for a multispectral image. **b** Reshaping the 2D image band *A* to a vector **a**

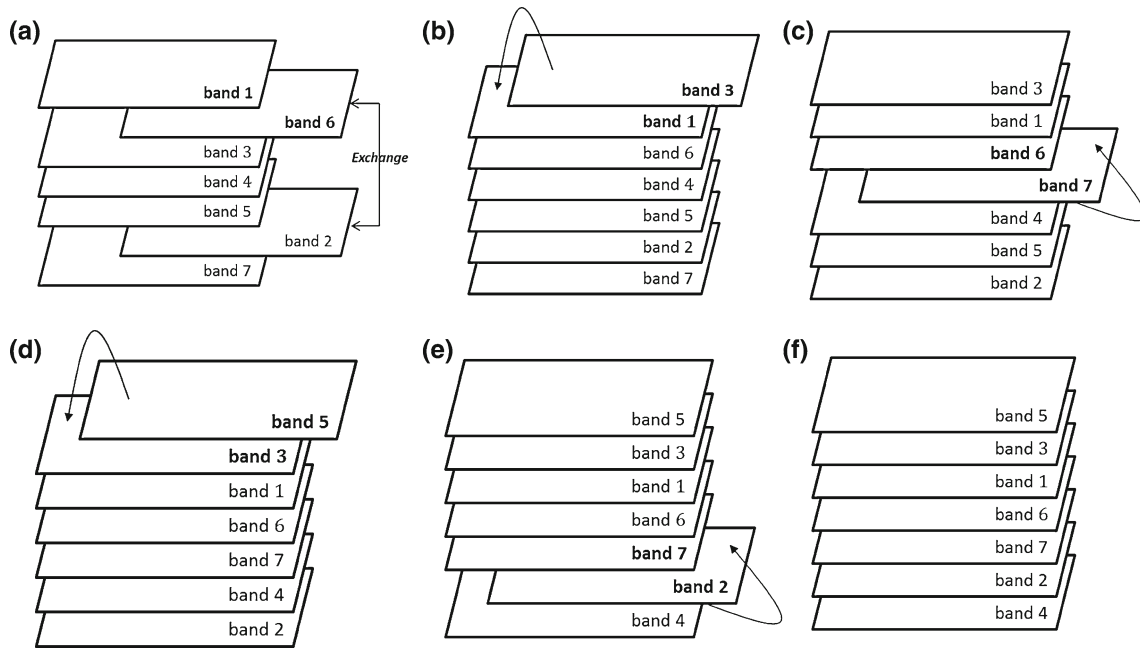
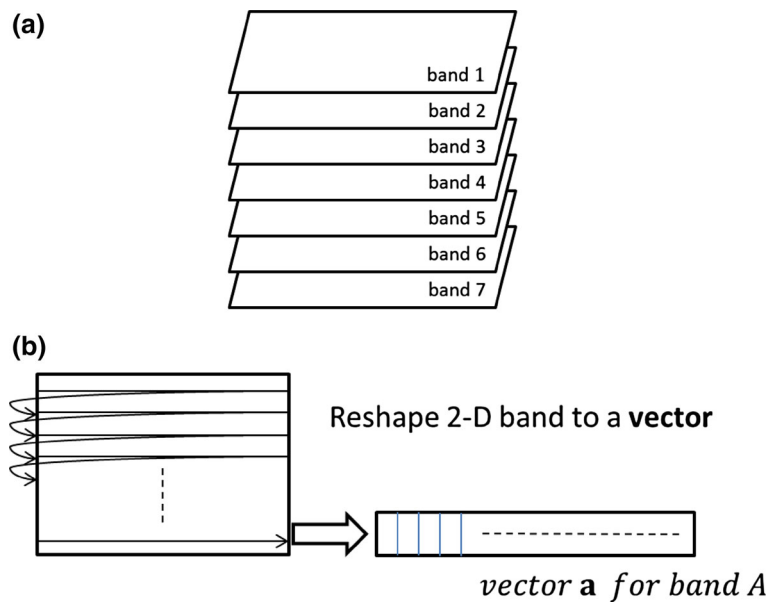


**Fig. 4** **a–e** The interchanges between bands. **f** Optimal multispectral band ordering

JPEG2000 supports the 9/7 floating point and the reversible 5/3 integer wavelet transforms. The 5/3 integer wavelet transform is based on the lifting scheme [18].

The scalar quantization is implemented with the quantization step size possibly varying for each sub-band. The Embedded Block Coding with Optimized Truncation (EBCOT) has two tiers. The first tier employs a context-based adaptive arithmetic coder called the MQ coder on each block of the sub-bands. The second tier is used for rate distortion optimization and quality layer formation. In [19], JPEG2000 is used for multispectral image compression.

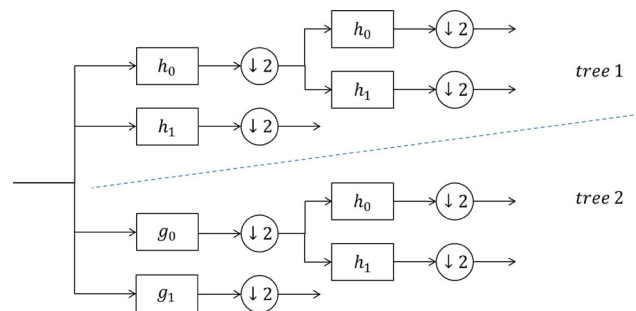
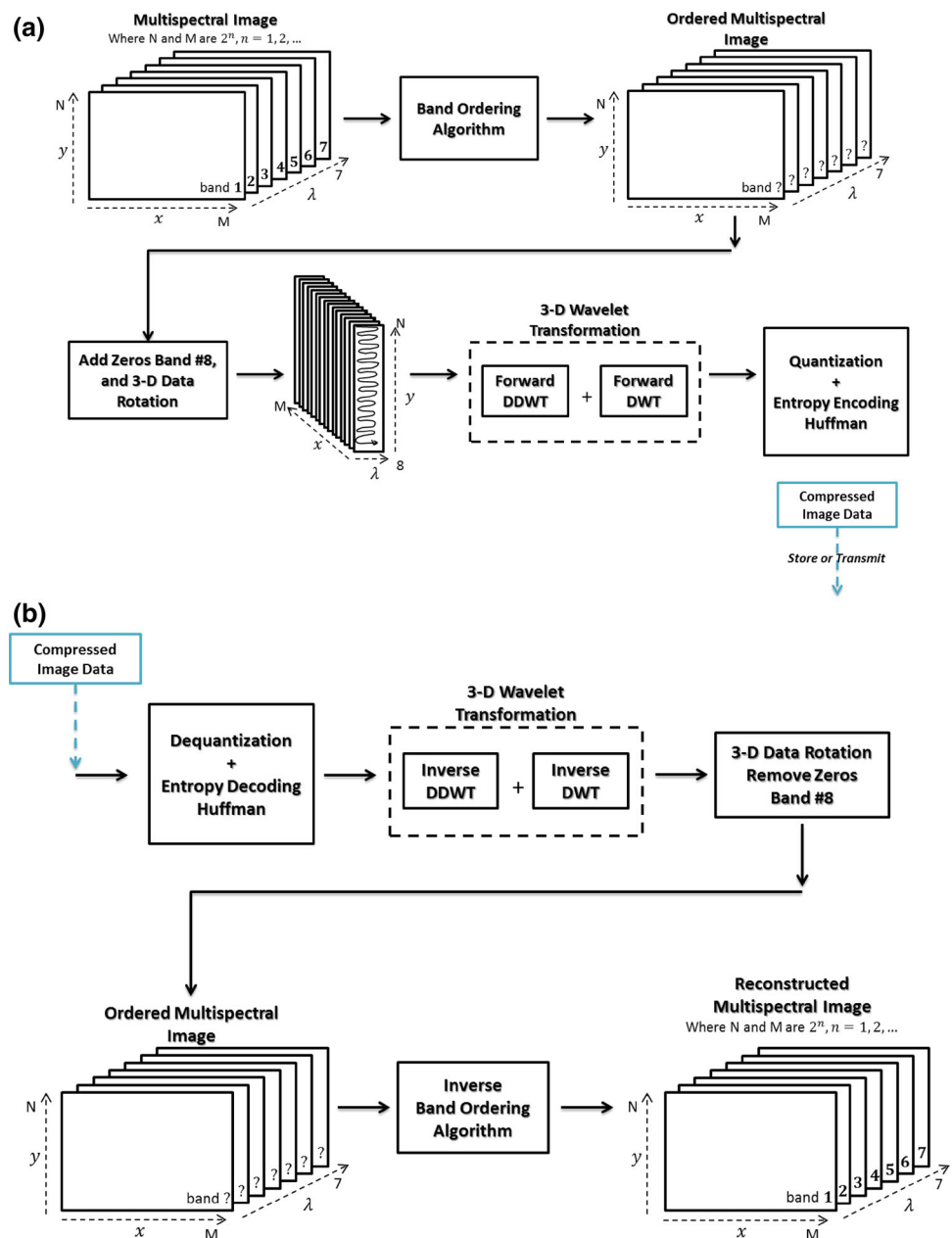


**Fig. 5** Analysis FB for the DDWT

**Fig. 6** **a** Block diagram for the proposed compression technique—encoder. **b** Block diagram for the proposed compression technique—decoder



#### 2.4 Compression with the 3D DDWT

The DDWT [12] is a relatively recent enhancement to the DWT with important additional properties. It is nearly shift-invariant and directionally selective in two and higher dimensions. It achieves this with a redundancy factor of only  $2D$  for  $D$ -dimensional signals, which is substantially lower than that of the undecimated DWT. The multidimensional ( $M$ -D) DDWT is non-separable, but it is based on a computationally efficient, separable filter bank (FB). The compression of spectral images with the 3D DDWT was discussed in [20]. To make the image spectral dimension even in the 3D transform, a new zero band (band #8) has to be added. The resulting

DDWT sub-bands are arranged in four separate transform combinations with each combination having the same sub-band organization as would a 3D DWT of the original data has but with each combination containing sub-bands of different orientations.

### 3 Proposed multispectral compression technique

In this section, we present an efficient multispectral image compression technique with high-quality reconstruction based on a multispectral band ordering, 3D DDWT in the spectral domain, and 2D DWT in the spatial domain.

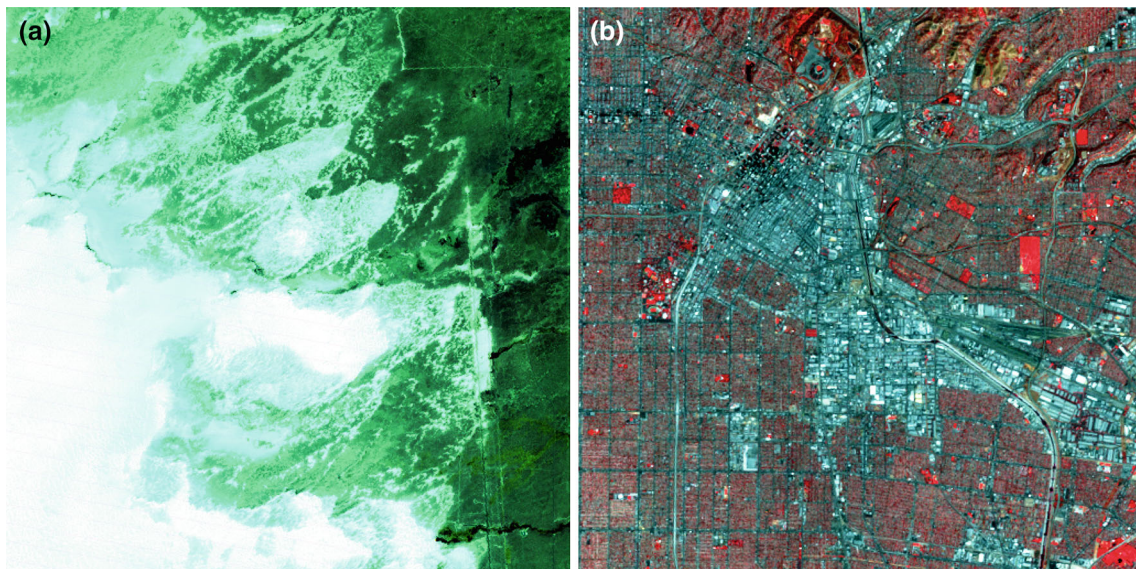


**Fig. 7** **a** Original multispectral images (bands 2, 3, and 4)—White Sands. **b** Original multispectral images (bands 2, 3, and 4)—Los Angeles

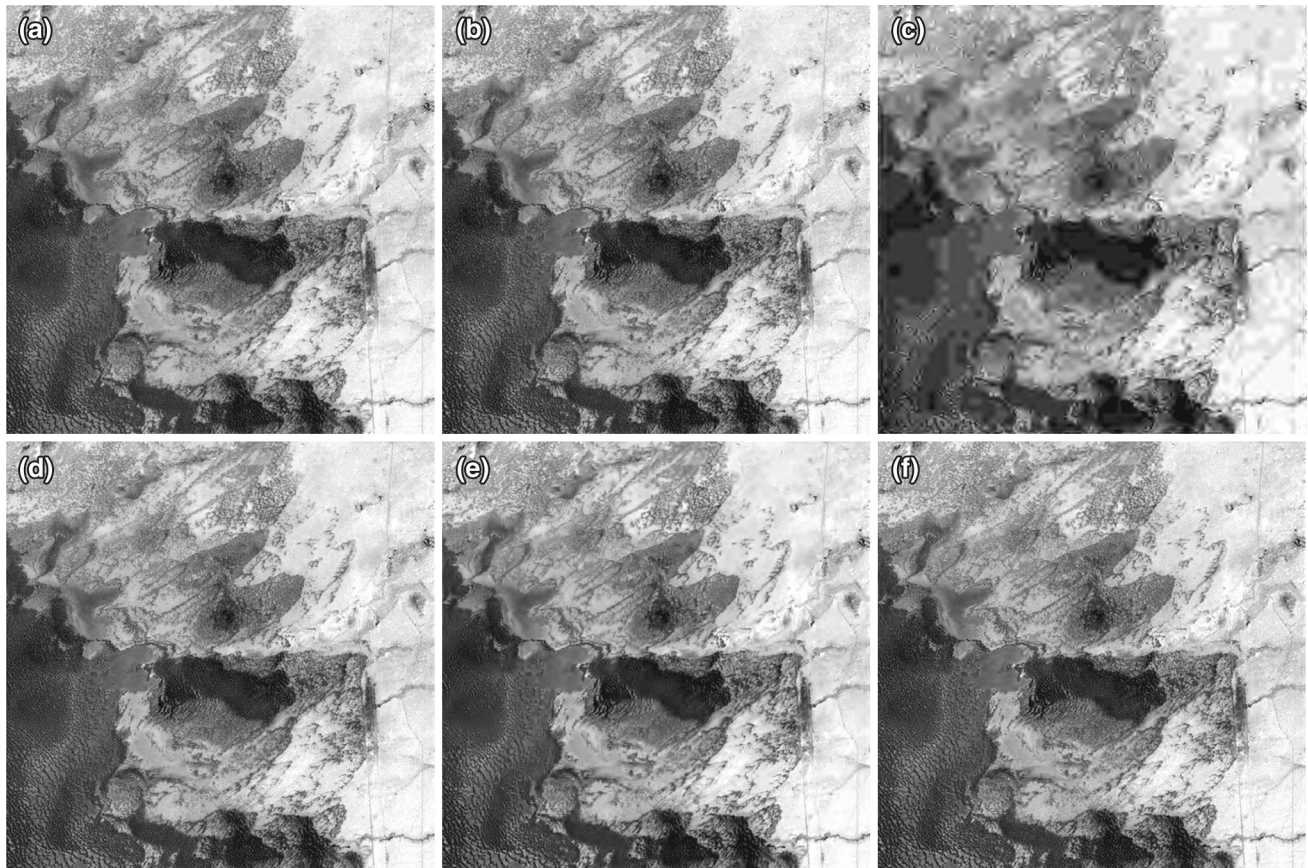


**Fig. 8** **a** White Sands image (Gray scale band #6) compression (CR  $\sim$  2.9)—original image band. **b** White Sands image (Gray scale band #6) compression (CR  $\sim$  2.9)—compressed band using JPEG. **c** White Sands image (Gray scale band #6) compression (CR  $\sim$  2.9)—compressed band using SPIHT. **d** White Sands image (Gray scale band #6) compression

(CR  $\sim$  2.9)—compressed band using JPEG2000. **e** White Sands image (Gray scale band #6) compression (CR  $\sim$  2.9)—compressed band using JPEG2000 with 3-D DDWT. **f** White Sands image (Gray scale band #6) compression (CR  $\sim$  2.9)—compressed band with the proposed technique

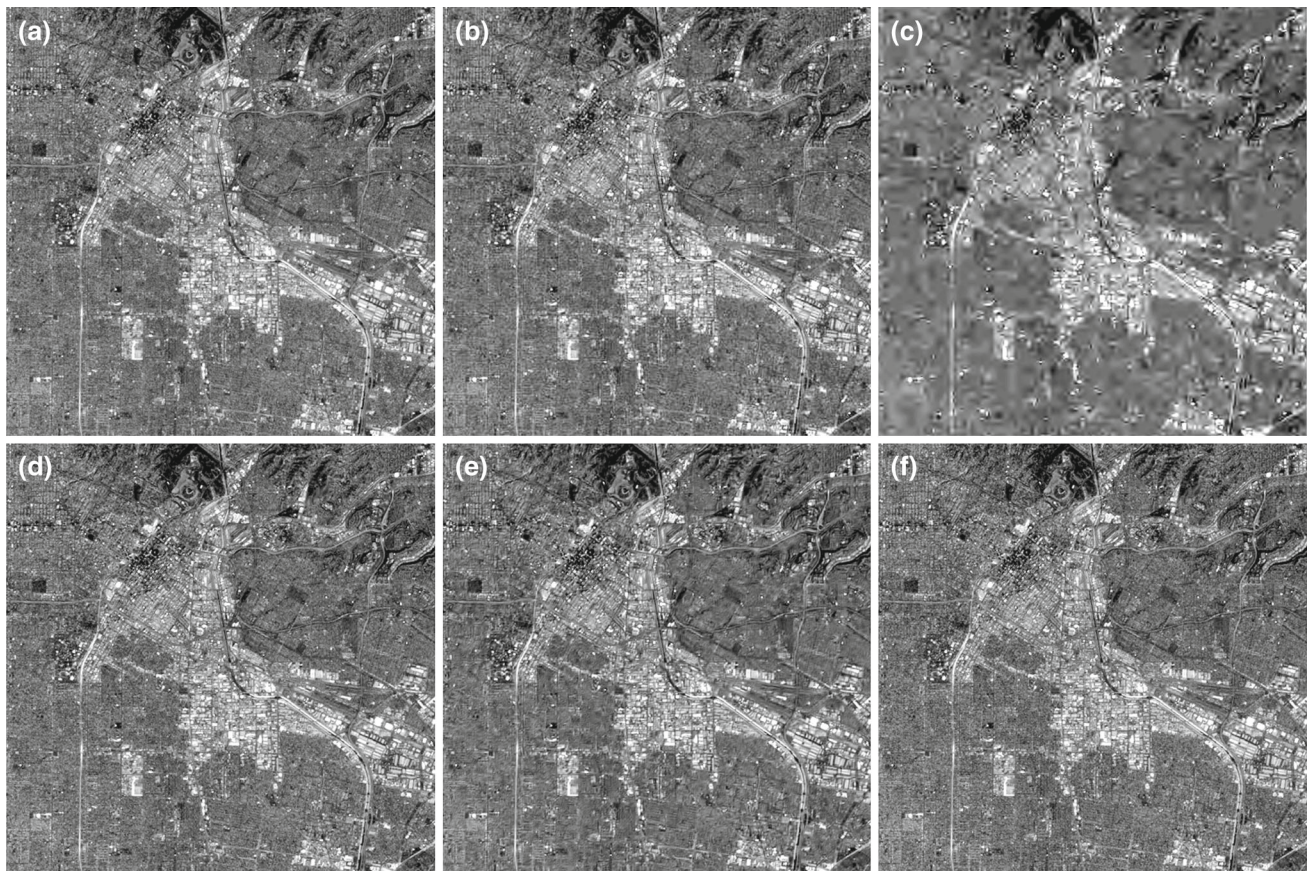


**Fig. 9** **a** Los Angeles image (Gray scale band #2) compression (CR  $\sim$  3.2)—original image band. **b** Los Angeles image (Gray scale band #2) compression (CR  $\sim$  3.2)—compressed band using JPEG. **c** Los Angeles image (Gray scale band #2) compression (CR  $\sim$  3.2)—compressed band using JPEG2000. **d** Los Angeles image (Gray scale band #2) compression (CR  $\sim$  3.2)—compressed band using SPIHT. **e** Los Angeles image (Gray scale band #2) compression (CR  $\sim$  3.2)—compressed band using JPEG2000 with 3D DDWT. **f** Los Angeles image (Gray scale band #2) compression (CR  $\sim$  3.2)—compressed band with the proposed technique

### 3.1 Multispectral band ordering

The proposed ordering heuristic uses the correlation coefficient to examine inter-band similarity. When a 3D image is split into a set of 2D bands, the inter-band similarity can be measured with the correlation coefficient due to its simplicity [6,21,22]. The correlation function takes two vectors as inputs and computes a real number in the range  $[-1.0, 1.0]$ , where 1.0 indicates that the input vectors are totally identical.

The correlation coefficient  $r_{A,B}$  between image bands  $A$  and  $B$  is calculated as follows [21]:

$$r_{A,B} = \frac{\sum_{j=0}^M \sum_{i=0}^N (A_{j,D,i,D} - \bar{A}) (B_{j,D,i,D} - \bar{B})}{\sqrt{\sum_{j=0}^M \sum_{i=0}^N (A_{j,D,i,D} - \bar{A})^2 \sum_{l=0}^M \sum_{k=0}^N (B_{l,D,k,D} - \bar{B})^2}} \quad (3)$$

where  $M$  is the number of rows and  $N$  is the number of columns in the image;  $\bar{A}$  and  $\bar{B}$  denote the mean values of the bands  $A$  and  $B$  computed for every  $D$ th pixel, respectively. Each  $D$ th pixel in the spatial directions is used for the computation of the correlation coefficients. If  $D$  equals

1, the exact value of the correlation between the two image bands is computed; otherwise, Eq. (3) results in a correlation estimate. The larger the  $D$ , the faster the reordering phase of the algorithm; however, at the same time, the estimation accuracy is reduced.

The proposed compression algorithm will be applied on Landsat ETM+ image with 7 bands. In the first step of this algorithm, the data of bands are reshaped to vectors as shown in Fig. 3. In the second step, Eq. (3) is applied for the image bands. The correlation coefficient between band #1 and band #2 is estimated as  $r_{1,2}$ , the correlation between band #1 and band #3 is estimated as  $r_{1,3}$ , and so on to obtain a vector of 21 values as  $[r_{1,2}, r_{1,3}, \dots, r_{1,7}, r_{2,3}, r_{2,4}, \dots, r_{2,7}, \dots, r_{6,7}]$ .

In the third step, the absolute values of the correlation vector are sorted in a descending order to determine the bands of the highest correlation bands. Finally, the bands are interchanged according to the correlation results to achieve the optimal band ordering for the multispectral image. For example, if we have the ordered values from the previous three steps as  $r_{1,6}, r_{1,3}, r_{1,5}, r_{6,7}, r_{3,5}, r_{3,4}$  and  $r_{2,7}$ , then band #1 and band #6 are conjugated as shown in Fig. 4a. After that,

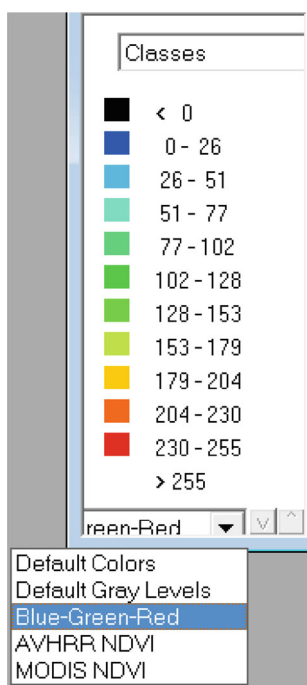


**Fig. 10** Snapshot for the Mulispec software that shows the thematic colors (blue–green–red) (color figure online)

band #1 and band #3 are conjugated as in Fig. 4b. The value  $r_{1,5}$  is omitted, because band #1 has the highest two correlations with bands #6 and #3. For  $r_{6,7}$ , band #6 and band #7 are conjugated as shown in Fig. 4c. Similarly, band #3 and band #5 are conjugated as in Fig. 4d. The value of  $r_{3,4}$  is omitted, because band #3 has the highest two correlation values with band #1 and band #5. Finally, Fig. 4e shows that band #2 and band #7 are conjugated. After band ordering, a data rotation step is performed to make the spectral dimension on the  $x$ -axis.

### 3.2 Wavelet transformation

The wavelet transform comes in several forms. The critically sampled form of the wavelet transform provides the most compact representation; however, it has several limitations. For example, it suffers severe shift dependence due to aliasing in down-samplers and the poor directional selectivity [20–27]. For these reasons, the DDWT is used in this paper as an alternative in the spectral dimension. Figure 5 illustrates the analysis FB for the DDWT. We apply the 2D DWT for the spatial dimension of the multispectral images, namely with Daubechies 9–7 filters [27].

### 3.3 Quantization and coding

After applying the DDWT on the spectral dimension and the DWT on the spatial dimension, a quantization process simi-

lar to that of the JPEG2000 standard is performed followed by Huffman coding [7, 8, 28, 29]. Figure 6 shows the block diagram for the proposed compression technique.

## 4 Experimental results

We have implemented the proposed compression technique on two multispectral image sets available on [30]; “White Sands, New Mexico May 9, 2000,” “Los Angeles, California, September 20, 1999”, Fig. 7.

We compared the proposed technique with JPEG, SPIHT, JPEG2000, and JPEG2000 with the 3D DDWT on different multispectral images.

Two experiments have been conducted and the results are shown in Figs. 8 and 9. In the former figure, band #6 is shown in gray scale for the White Sands image with different compression methods. Figure 9 shows band #2 in gray scale for the original Los Angeles image with different compression methods.

The thematic colors with blue–green–red representation are shown in Fig. 10 using the specific multispectral analysis software [31]. Figure 11 shows Los Angeles band #5 compressed with different compression techniques.

The performance of the compression methods has been studied and distortion metrics such as the mean square error (MSE) and the peak signal-to-noise ratio (PSNR) are considered.

Let  $0 \leq g(i, j, k) \leq g_{fs}$  denote an  $N$ -pixel digital image in band  $k$  for a multispectral image ( $N \times M \times \lambda$ ),  $g_{fs}$  is the largest pixel and let  $\bar{g}(i, j, k)$  be its possibly distorted version obtained by compressing  $g(i, j, k)$  and decompressing the output bit stream, the  $MSE$  and the  $PSNR$  are defined as:

$$MSE = \frac{1}{NM} \sum_{k=1}^{\lambda} \sum_{i=0}^{N-1} \sum_{j=0}^{M-1} [g(i, j, k) - \bar{g}(i, j, k)]^2 \tag{4}$$

$$PSNR = \frac{20}{\lambda} \sum_{k=1}^{\lambda} \log_{10} \frac{g_{fs}}{\sqrt{MSE_k}} \tag{5}$$

where  $\lambda$  is the number of bands and  $MSE_k$  is the MSE for band  $k$ .

Spectral distortion metrics such as the spectral angle mapper (SAM) and the spectral information divergence (SID) are also considered for the comparison purpose [32]. Given two spectral vectors  $\mathbf{V}$  and  $\tilde{\mathbf{V}}$  both having  $L$  components, let  $\mathbf{V} = \{v_1, v_2, \dots, v_L\}$  be the original spectral pixel vector  $v_l = g_l(i, j)$  and  $\tilde{\mathbf{V}} = \{\tilde{v}_1, \tilde{v}_2, \dots, \tilde{v}_L\}$  its distorted version obtained after compression and decompression. Analogous to the radiometric distortion metrics, spectral distortion metrics may be defined.

**Fig. 11** **a** Los Angeles image (Thematic band #5) results—original image band. **b** Los Angeles image (Thematic band #5) results—the compressed band with JPEG2000. **c** Los Angeles image (Thematic band #5) results—the compressed band with SPIHT. **d** Los Angeles image (Thematic band #5) results—the compressed band with the proposed technique

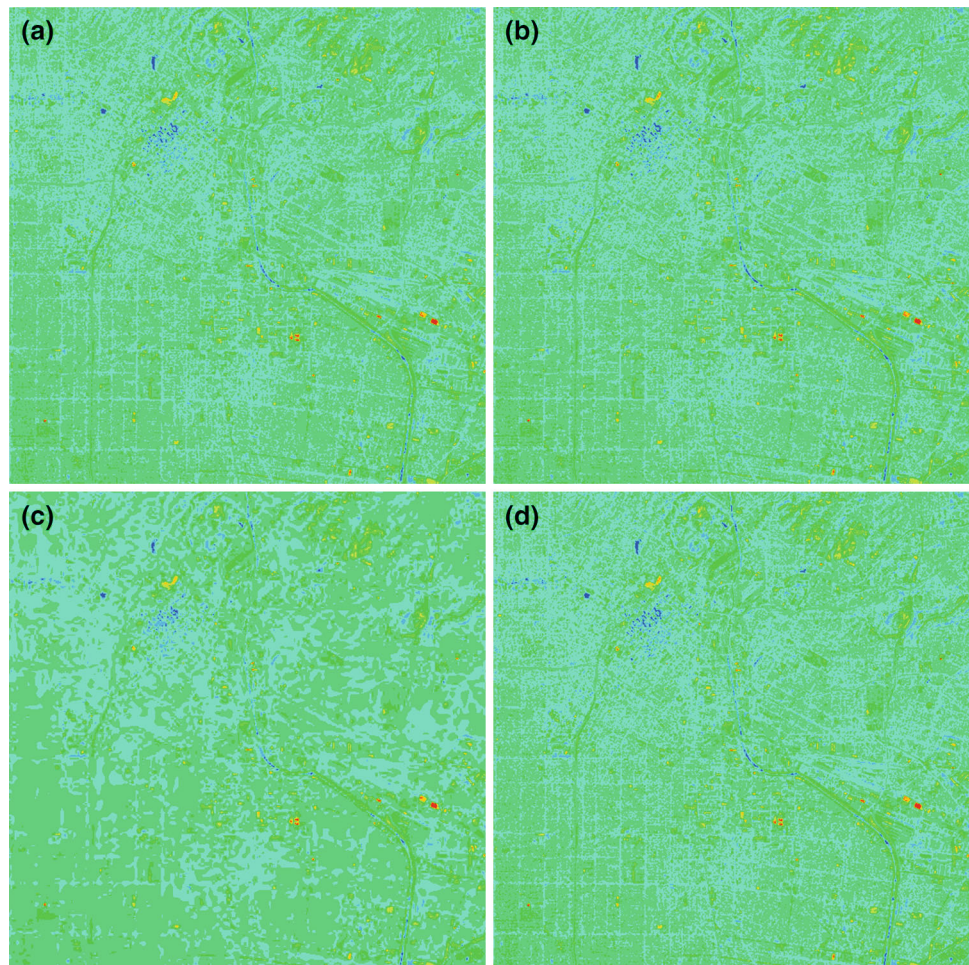


**Table 1** MSE and PSNR values for the two images with and without band ordering and 3D rotation

| Image               | Without band ordering and 3D rotation |       |           | With band ordering and 3D rotation |       |           |
|---------------------|---------------------------------------|-------|-----------|------------------------------------|-------|-----------|
|                     | CR                                    | MSE   | PSNR (dB) | CR                                 | MSE   | PSNR (dB) |
| Image1: White Sands | 2.8                                   | 20.70 | 43.54     | 2.8                                | 19.48 | 43.95     |
|                     | 3.3                                   | 33.44 | 41.50     | 3.4                                | 32.00 | 41.85     |
|                     | 4.2                                   | 57.07 | 39.22     | 4.2                                | 50.52 | 39.90     |
|                     | 5.0                                   | 76.97 | 37.91     | 5.1                                | 72.69 | 38.32     |
| Image2: Los Angeles | 2.8                                   | 19.59 | 43.82     | 3.2                                | 16.65 | 44.55     |
|                     | 3.4                                   | 35.72 | 41.22     | 3.8                                | 27.53 | 42.48     |
|                     | 4.3                                   | 61.89 | 38.86     | 4.6                                | 44.56 | 40.53     |
|                     | 5.1                                   | 84.58 | 37.52     | 5.9                                | 75.75 | 38.28     |

SAM denotes the absolute value of the spectral angle between the couple of vectors calculated as [6]:

$$\text{SAM}(\mathbf{V}, \tilde{\mathbf{V}}) = \arccos\left(\frac{\langle \mathbf{V}, \tilde{\mathbf{V}} \rangle}{\|\mathbf{V}\|_2 \cdot \|\tilde{\mathbf{V}}\|_2}\right) \quad (6)$$

in which  $\langle \cdot, \cdot \rangle$  stands for scalar product.

The SID is derived from information-theoretic concepts as [32]:

$$\text{SID}(\mathbf{V}, \tilde{\mathbf{V}}) = \sum_{l=1}^L (p_l - q_l) \log\left(\frac{p_l}{q_l}\right) \quad (7)$$

where

$$p_l = \frac{v_l}{\|\mathbf{V}\|_1}, \text{ and } q_l = \frac{\tilde{v}_l}{\|\tilde{\mathbf{V}}_1\|} \quad (8)$$

Table 1 tabulates the MSE and PSNR values for the proposed compression technique with and without band ordering



**Table 2** MSE and PSNR values for the two images compressed with different compression techniques

| Methods                | Image1: White Sands |           | Image2: Los Angeles |           |
|------------------------|---------------------|-----------|---------------------|-----------|
|                        | MSE                 | PSNR (dB) | MSE                 | PSNR (dB) |
| JPEG                   | 79.74               | 38.71     | 98.37               | 37.86     |
| SPIHT                  | 181.28              | 34.80     | 303.36              | 32.58     |
| JPEG2000               | 26.04               | 42.89     | 33.01               | 41.47     |
| JPEG2000 with 3-D DDWT | 34.71               | 41.41     | 52.37               | 39.58     |
| Proposed               | 19.48               | 43.95     | 16.65               | 44.55     |

**Table 3** SAM and SID values for the images compressed with different compression techniques

| Methods                | Image1: White Sands |         | Image2: Los Angeles |         |
|------------------------|---------------------|---------|---------------------|---------|
|                        | SAM                 | SID     | SAM                 | SID     |
| JPEG                   | 0.923               | 0.27E−3 | 1.832               | 0.17E−2 |
| SPIHT                  | 1.266               | 0.59E−3 | 2.978               | 0.30E−2 |
| JPEG2000               | 0.592               | 0.97E−4 | 1.163               | 0.52E−3 |
| JPEG2000 with 3-D DDWT | 0.592               | 0.26E−3 | 1.451               | 0.71E−3 |
| Proposed               | 0.317               | 0.75E−4 | 0.775               | 0.25E−3 |

and 3D rotation. The results in this table are in favor of band ordering and 3D rotation. Table 2 shows the MSE and PSNR values for the different compression techniques including the proposed one. The results in the table are in favor of the proposed technique. Table 3 shows the SAM and SID values for the different compression techniques. These results also are in favor of the proposed compression technique.

## 5 Conclusion

An efficient multispectral image compression technique with optimal band ordering has been proposed in this paper. It is based on the multispectral band ordering, the 3D DDWT, the 2D DWT, and a simple Huffman coder. We take full advantage of the multispectral bands in the step of band ordering and in the transformation by using the DDWT on the spectral dimension and the DWT on the spatial dimension. From the subjectivity and objectivity, we can conclude that the proposed compression technique is more effective than other traditional compression techniques.

## References

- Salomon, D.: Data Compression, the Complete Reference, 4th edn. Springer, Berlin (2007)
- NASA: The Landsat Program. <http://landsat.gsfc.nasa.gov/>. Accessed 28 Jan 2012
- U. G. Service: Landsat missions. <http://landsat.usgs.gov/>. Accessed 28 Jan 2012
- Delcourt, J., Mansouri, A., Sliwa, T., Voisin, Y.: A comparative study and an evaluation framework of multi/hyperspectral image compression. *IEEE* (2009). doi:10.1109/SITIS
- Yaw, C., Paramesran, R., Mukundan, R., Jiang, X.: Image quality assessment by discrete orthogonal moments. *Pattern Recognit.* **43**(12), 4055–4068 (2010)
- Motta, G., Rizzo, F., Storer, J.: *Hyperspectral Data Compression*, 2006 Edition, Springer, Science and Business Media, public, Berlin (2005)
- ISO/IEC 15444-1. Information technology. JPEG2000 image coding system-part 1: core coding system (2005)
- Skodras, A., Christopoulos, C., Ebrahimi, T.: The JPEG 2000 still image compression standard. *IEEE Signal Process. Mag.* **18**(5), 36–58 (2001)
- Dragotti, P.L., Poggi, G., Ragozini, A.: Compression of multispectral images by three-dimensional SPIHT algorithm. *IEEE Trans. Geosci. Remote Sens.* **38**(1), 416–428 (2000)
- Said, A., Pearlman, W.: A new fast and efficient image codec based on set partitioning in hierarchical trees. *IEEE Trans. Circuits Syst. Video Technol.* **6**, 243–250 (1996)
- Wright, D., Harris, F.: The JPEG algorithm for image compression: a software implementation and some test results. In: *Conference Record of the Twenty-Fourth Asilomar Conference on Signals, Systems and Computers* (1990)
- Selesnick, I., Baraniuk, R., Kingsbury, N.: The dual-tree complex wavelet transform. *IEEE Signal Process. Mag.* **22**(6), 123–151 (2005)
- Ahmed, N., Natarajan, N., Rao, K.R.: Discrete cosine transform. *IEEE Trans. Comput.* **C-23**(1), 90–93 (1974)
- Duttweiler, L., Chamzas, C.: Probability estimation in arithmetic and adaptive-Huffman entropy coders. *IEEE Trans. Image Process.* **4**(3), 237–246 (1995)
- Pellegrini, P., Novati, G., Schettini, R.: Multispectral loss-less compression using approximation methods. *IEEE*. 0-7803-9134-9/05 (2005)
- Saghri, J., Tescher, A., Reagan, J.: Practical transform coding of multispectral imagery. *IEEE Signal Process. Mag.* **12**(1), 32–43 (1995)

17. Chung, L., Chen, K., Chen, H., Chen, L.: Analysis and architecture design of block-coding engine for EBCOT in JPEG 2000. *IEEE Trans. CSVT* **13**(3), 219–230 (2003)
18. Shapiro, J. M.: Apparatus and method for compressing information. United States Patent Number 5,412,741. Issued 2 May 1995
19. Wei, J., Wei, R., Gao, X., Duan, X.: Multispectral images compression based on JPEG2000. *IEEE, SIBGRAP'05*. 1530-1834/05 (2005)
20. Boettcher, J., Du, Q.: Hyperspectral image compression with the 3D dual-tree wavelet transform. *IEEE* (2007). doi:[10.1109/IGARSS](https://doi.org/10.1109/IGARSS)
21. Toivanen, P., Kubasova, O., Mielikainen, J.: Correlation-based band-ordering heuristic for lossless compression of hyperspectral sounder data. *IEEE Geosci. Remote Sens. Lett.* **2**(1), 50–54 (2005)
22. Tate, S.: Band ordering in lossless compression of multispectral images. *IEEE Trans. Comput.* **46**(4), 477–483 (1997)
23. Fang, Z., Luo, G., Liu, Z., Gan, Y., Lu, Y.: Multi-spectral image compression technology based on dual-tree discrete wavelet transform. *Proceedings of SPIE*, vol. 7494, *Multispectral Image Acquisition and Processing* (2009)
24. Selesnick, I.W.: The double-density dual-tree DWT. *IEEE Trans. Signal Process.* **52**(5), 1304–1314(2004)
25. Kingsbury, N.: Image processing with complex wavelets. *Phil. Trans. R. Soc. Lond. A* **357**(1760), 2543–2560 (1999)
26. Poularikas, A.D.: *The Handbook of Formulas and Tables for Signal Processing*. Springer, and CRC Press LLC, Berlin (1999)
27. Antonini, M., Barlaud, M., Mathieu, P., Daubechies, I.: Image coding using wavelet transform. *IEEE Trans. Image Process.* **1**(2), 205–220 (1992)
28. Gonzalez, R.C., Woods, R.E.: *Digital Image Processing*, 3rd edn. Prentice Hall, Pearson Education, Englewood Cliffs, NJ (2007)
29. Gonzalez, R., Eddins, S., Woods, R.: *Digital Image Processing Using Matlab*, 1st edn. Prentice Hall, Pearson Education, Englewood Cliffs, NJ (2003)
30. Online Sources. Available: <http://17downloads.gsfc.nasa.gov/index.htm>. Accessed 18 July 2012
31. MultiSpec Software. Available: <https://engineering.purdue.edu/~biehl/MultiSpec/>. Accessed 04 May 2012
32. Chang, C.I.: An information-theoretic approach to spectral variability, similarity, and discrimination for hyperspectral image analysis. *IEEE Trans. Inf. Theory* **46**(5), 1927–1932 (2000)